

OMAE2009-79766

A COMPARISON BETWEEN CFD, POTENTIAL THEORY AND MODEL TESTS FOR OSCILLATING AIRCUSHION SUPPORTED STRUCTURES

J.L.F. van Kessel

*Offshore Engineering Department,
Delft University of Technology,
Delft, The Netherlands*

F. Fathi

*GustoMSC
Schiedam, The Netherlands*

ABSTRACT

This contribution presents a comparison between Computational Fluid Dynamics (CFD), potential theory and model tests for an oscillating aircushion supported structure.

The linear method was developed at Delft University of Technology and uses a linear adiabatic law to describe the air pressure inside the cushion. In this method, the structure and the water surface within the aircushion are modelled by means of panel distributions representing oscillating sources.

The CFD solver is the commercial software CFX which solves the whole flow field using Reynolds Averaged Navier Stokes Equations (RANSE). The free surface is modelled by a Volume of Fluid (VOF) approach.

The results in this paper show a good agreement between experimental results and numerical results of both methods for aircushion pressure variations, added mass, damping and wave elevations inside the aircushion.

As such it is validated that the behaviour of an aircushion supported structure subjected to forced heave oscillations can be well predicted by both CFD and potential theory.

KEYWORDS

Aircushion supported structure, model tests, potential theory, CFD, forced oscillations, added mass, damping, air pressure variations, wave elevation.

INTRODUCTION

Aircushions can significantly influence the behaviour of large floating offshore structures in waves. Research in the past has shown that aircushions can be of particular interest for large floating offshore structures since wave bending moments and drift forces can both be significantly reduced at the same time.

The behaviour of large aircushion supported structures in waves was studied by Pinkster et. al. [12] - [15] and Van Kessel et. al. [21] - [25] at Delft University of Technology. Tabeta carried out model tests in the towing tank of the Ship Hydrodynamics Laboratory which served as a validation of the computational method [17]. In addition, Pinkster and Meevers Scholte [15], [20] performed model experiments of a large aircushion supported Mobile Offshore Base (MOB) at the same facility in 1999.

Lee and Newman [10] carried out computations with respect to acoustic disturbances in an aircushion. Thiagarajan et. al. [18] investigated the wave-induced motions of air-supported offshore structures in shallow water by means of an analytical approach and model tests. Ikoma et. [2 - 9] al. investigated the behaviour of aircushions on floating structures at the College of Science and Technology at Nihon University, this research was mainly aimed at investigating the effects of air chambers on the hydroelastic response of floating structures. Tsubogo et. al. [19] used a different numerical approach to calculate the behaviour of an elastic aircushion supported structure. In his case the air inside the cushion was also described by a potential formulation.

The present contribution describes the use of a CFD method for aircushion supported structures. In addition a comparison with potential theory and model tests will be given. First, both numerical methods will be introduced, followed by a description of the model tests program. Afterwards, the numerical and experimental results will be discussed and finally conclusions will be drawn.

THEORETICAL FORMULATION

Both CFD and potential computations were performed in order to compute the behaviour of an aircushion supported structure subjected to forced heave oscillations. CFD computations were performed with the program ANSYS-CFX version 11.0. First the basic theory underlying these computations will be discussed in this section. Next a description of the potential theory will be given.

CFD METHOD

Computational Fluid Dynamics (CFD) simulates the viscous flow field in the whole domain. For each grid cell, the fluid velocity vector and the pressure scalar are computed at each time step. In this paper, the time dependent incompressible Navier-Stokes equations are solved in their statistical Reynolds averaged (URANS) formulation [26].

The CFD solver ANSYS-CFX [1] uses a finite volume discretization on a collocated grid of the URANS equations to determine the time evolution of the flow field. The presence of both air and water in the simulation is modeled by the volume of fluid (VOF) method. Within each cell, the relative proportion of each phase is given by the volume fraction ϕ . This scalar function comprised between 0 (grid cell full of air) and 1 (cell full of water) is used as a weighting function. A unique flow field is solved by the URANS equations where the relative contribution of each phase is represented by ϕ for water and $(1 - \phi)$ for air. The time evolution of ϕ is given by the transport equation, Eq. (1). The free surface profile, generally defined as the iso-surface with constant $\phi=0.5$ is sharpened using a specific compression algorithm as described in [1]. Both air and water are modeled as incompressible fluids. The fluid equations solved by the code are the following:

$$\begin{aligned} \frac{\partial \bar{V}_i}{\partial x_i} &= 0 \\ \frac{\partial \bar{V}_i}{\partial t} + \frac{\partial}{\partial x_j} (\bar{V}_i \bar{V}_j) &= -\frac{1}{\rho} \left[\frac{\partial \bar{p}}{\partial x_i} + \mu_0 \frac{\partial}{\partial x_j} \left(\frac{\partial \bar{V}_i}{\partial x_j} + \frac{\partial \bar{V}_j}{\partial x_i} \right) + R_{ij} \right] + F_V \quad (1) \\ \frac{\partial \phi}{\partial t} + \bar{V}_i \frac{\partial \phi}{\partial x_i} &= 0 \\ \rho &= \phi \rho_{water} + (1 - \phi) \rho_{air} \\ \mu_0 &= \phi \mu_{water} + (1 - \phi) \mu_{air} \\ i &= x, y, z \end{aligned}$$

in which:

$$\begin{aligned} \bar{V}_i &= i \text{ component of the statistically averaged} \\ &\text{velocity} \\ \rho &= \text{fluid mixture density} \\ F_V &= \text{Buoyancy force} \\ R_{ij} &= \text{Reynolds stress tensor} \end{aligned}$$

The URANS formulation implies a closure modeling of the averaged cross products of the fluctuating terms which are not solved by the averaged equations, known as Reynolds stresses R_{ij} .

A classical 2-equation eddy viscosity model, Menter's Shear Stress Transport (SST) is employed in this respect [11].

Following Boussinesq's assumption, the Reynolds stresses are considered proportional to the fluid shear stresses.

$$R_{ij} = -\mu_t \frac{\partial}{\partial x_j} \left(\frac{\partial \bar{V}_i}{\partial x_j} + \frac{\partial \bar{V}_j}{\partial x_i} \right) + \frac{2}{3} \delta_{ij} k \quad (2)$$

in which:

$$\begin{aligned} k &= \text{turbulent kinetic energy} \\ \mu_t &= \text{turbulent viscosity} \end{aligned}$$

The turbulent viscosity is an anisotropic model for the added energy dissipation occurring in the fluid because of turbulence. Its effect is then taken into account by simply adding it to the fluid viscosity μ_0 . μ_t is determined locally by solving two more scalar equations corresponding to the fields of turbulent kinetic energy k and turbulent dissipation frequency ω . μ_t is then retrieved using the dimensional relation $\mu_t = \rho k / \omega$. The complete formulation can be found in [11].

CFX uses a multi-grid accelerated algorithm [16] to solve both the continuity equation and the momentum equations in a single system. Non-linearities of the system are treated using an iterative pseudo-transient approach.

3D POTENTIAL METHOD

The rigid part of the aircushion supported structure is modelled in the usual way by means of panels representing pulsating sources distributed over the mean wetted surface of the construction. The free surface within the aircushion is modelled by panels representing oscillating source distributions laying in the mean free surface of the cushion.

All panels of the free surface within an aircushion are assumed to represent a body without material mass but having added mass, damping, hydrostatic restoring and aerostatic restoring characteristics. Each free surface panel has one degree of freedom being the vertical motion of panel n within cushion c . It will be clear that properties such as added mass coupling and damping coupling exist between all free surface panels and the rigid part of the construction. The total number of degrees of freedom (*D.O.F.*) therefore amounts to:

$$D.O.F. = 6 + \sum_{c=1}^C N_c \quad (3)$$

in which:

$$N_c = \text{number of panels in cushion } c$$

The number 6 represents the six degrees of freedom of the rigid part of the structure. The equations of motion for an aircushion supported structure can be written as:

$$\sum_{j=1}^{D.O.F.} \left\{ -\omega^2 (M_{nj} + a_{nj}) - i \omega b_{nj} + c_{nj} \right\} x_j = X_n, \quad n=1, 2, \dots, D.O.F. \quad (4)$$

in which:

- M_{nj} = mass coupling coefficient for the force in the n -mode due to acceleration in the j -mode. Zero for cushion panels.
- a_{nj} = added mass coupling coefficient
- b_{nj} = damping coupling coefficient
- c_{nj} = spring coupling coefficient
- x_j = mode of motion
- \dot{X}_n = wave force in the n -mode

In the above equation $j=1,6$ and $n=1,6$ represent motions and force modes respectively of the rigid part of the structure. The case of $j>6$ and $n>6$ represents the coupling between the panels of the free surfaces of the aircushions. The case of $j=1,6$ and $n>6$ represents the coupling between the rigid part of the construction and the vertical forces of the free surface panels in the cushions. $j>6$ and $n=6$ represents the coupling between vertical motions of the free surface panels in the aircushions and the six force modes on the rigid part of the structure.

The wave force X_n , the added mass and damping coupling coefficients a_{nj} and b_{nj} are determined in the same way as is customary for a multi-body system. The contribution to the total potential due to the discrete pulsating source distributions over the structure and the free surface of the aircushions can be expressed as:

$$\phi_j(\bar{X}) = \frac{1}{4\pi} \sum_{s=1}^{N_c} \sigma_{sj}(\bar{A}) G(\bar{X}, \bar{A}) \Delta S_s \quad (5)$$

in which:

- N_c = total number of panels of the structure and free surfaces of all cushions
- \bar{X} = X_1, X_2, X_3 = a field point
- \bar{A} = A_1, A_2, A_3 = location of a source
- $G(\bar{X}, \bar{A})$ = Green's function of a source in \bar{A} relative to a field point \bar{X}
- ΔS_s = surface element of the body or the mean free surfaces in the aircushions
- σ_{sj} = strength of a source on surface element s due to motion mode j
- $\phi_j(\bar{X})$ = potential in point \bar{X} due to j -mode of motion

The unknown source strengths σ_{sj} are determined based on boundary conditions placed on the normal velocity of the fluid at the centres of the panels:

$$-\frac{1}{2} \sigma_{mj}(\bar{X}) + \frac{1}{4\pi} \sum_{s=1}^{N_c} \sigma_{sj}(\bar{A}) \frac{\partial}{\partial n} G(\bar{X}, \bar{A}) \Delta S_s = \frac{\partial \phi_j}{\partial n_m}, \quad m=1, 2, \dots, N_t \quad (6)$$

The right hand side of the above equation depends on the case to be solved.

Added mass and damping coupling coefficients are found by applying normal velocity requirements. For the six rigid body motions ($j=1,6$) of the structure:

$$\frac{\partial \phi_j}{\partial n_m} = n_{mj} \quad j=1, 6 \quad (7)$$

For this case the normal velocity components on all cushions panels are equal to zero.

For the determination of the added mass and damping coupling arising from the normal motions of individual cushion panels the normal velocity boundary condition is zero except for one cushion panel at a time for which the following value holds:

$$\frac{\partial \phi_m}{\partial n_m} = -1 \quad (8)$$

where the -1 follows from the fact that the free surface normal is pointing in the negative X_3 -direction.

From the solutions of the source strengths for all these cases the total added mass a_{nj} and damping coupling coefficients b_{nj} can be obtained:

$$a_{nj} = -\text{Re} \left[\rho \sum_{k=1}^{N_n} \phi_{j,k} n_{n,k} \Delta S_{n,k} \right] \quad (9)$$

$$b_{nj} = -\text{Im} \left[\rho \omega \sum_{k=1}^{N_n} \phi_{j,k} n_{n,k} \Delta S_{n,k} \right]$$

in which:

- N_n = number of panels involved in the force in the n -mode. For the force on a cushion panel $N_n = 1$. For the force on the structure $N_n = N_s$
- n_{nk} = generalised directional cosine of k -panel related to n -mode
- ΔS_{nk} = area of k -panel related to the force in the n -mode
- $\phi_{j,k}$ = motion potential value on k -panel obtained from Eq. (5)

The restoring coefficients c_{nj} in general consist of two contributions i.e. an aerostatic spring term and a hydrostatic spring term as described in [21]. The hydrostatic restoring term is equal to the product of the waterline area, specific mass water and acceleration of gravity. This applies to both the structure and the free surface panels. The aerostatic restoring terms are related to the change in air pressure in an aircushion due to, for instance, unit vertical displacement of a free surface panel. Conversely, displacing the structure in any of the three vertical modes of heave, roll or pitch may change the volume of an aircushion as well, thus inducing pressure changes resulting in forces on all free surface panels and the structure.

For the determination of the aerostatic part of the restoring terms, use is made of a linearized adiabatic law as described in [21].

The motions of the cushion panels due to oscillations of the structure are determined by solving the equation of motion for all individual panels. Use is made of added mass and damping coupling coefficients, as well as spring coupling coefficients based on the aerostatic restoring coefficients and the hydrostatic restoring coefficients of the cushion panels:

$$\sum_{j=1}^6 \{-\omega^2 a_{ij} - i\omega b_{ij} + c_{ij}\} x_j = X_n, \quad n=7, D.O.F. \quad (10)$$

From the solution of the equation of motion of the cushion panels the cushion pressure variations and the total added mass and damping coefficients for the aircushion supported structure can be obtained.

NUMERICAL SETTINGS AND EXPERIMENTAL SETUP

Results of model tests performed by Tabeta [17] will be used to validate the results of the CFD and potential method. This section describes the main particulars of the experimental model, and numerical models used for CFD and potential computations.

MODEL TESTS

Forced heave oscillation tests were performed by Tabeta [17] in towing tank No.1 of the Ship Hydrodynamics Laboratory of Delft University of Technology. This facility measures 140 m x 4.25 m x 2.5 m. It is equipped with a hydraulically operated, flap-type wave maker, by means of which regular or irregular waves can be generated.

A simple rectangular barge model measuring 2.50 m x 0.70 m x 0.50 m was constructed out of wood. The model consisted of a horizontal deck surrounded by vertical side walls. The draft of the barge measured to the lower edge of the side walls was equal to 0.30 m. The thickness of the deck plate and the walls surrounding the aircushion was 2.0 cm. The main particulars of the model are presented in Table 1.

Table 1: Main particulars of the aircushion model

Length	m	2.50
Breadth	m	0.70
Draught (structure)	m	0.30
Draught (cushion)	m	0.15
Area of Water Line	m ²	1.75
Displacement	m ³	0.2815
Oscillating Mass	kg	160

Forced heave oscillations with amplitudes of 1 cm and 2 cm were carried out in the basin. During these oscillations, the

heave added mass and damping coefficients were measured, as well as the cushion pressure variations and the water elevation inside the cushion.

Figure 1 shows the test set-up and location of the measuring devices. The cushion pressure variations are measured at locations P_1 and P_2 and the water elevation (ζ_b) is measured at $(x, y) = (0.1 \text{ m}, 0.0 \text{ m})$.

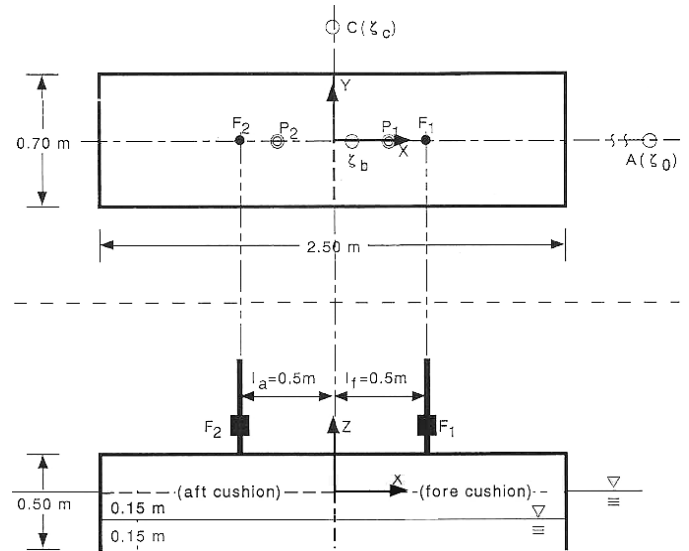


Figure 1: Setup of the model tests

CFD METHOD

Forced oscillation tests are simulated by imposing a harmonically periodic motion to the aircushion supported structure in still water. In order to save computational resources, the problem is reduced to two dimensions. Only the transverse section of the cushion is modeled and 3D effects are neglected. A multi-block body fitted structured mesh is generated using the software ANSYS-ICEM as shown in Figure 2. Even if CFX makes use of unstructured grids only, the multi-block approach is preferable due to a better alignment with the flow of the grid cells when compared to the unstructured tetrahedral mesh generation. The regularity of the cell distribution is also an advantage when considering the mesh deformation caused by the cushion displacement. Indeed, the cushion is modeled as an oscillating solid wall boundary around which the mesh will deform according to the cushion displacement. The near wall flow is captured by an O-grid structure of the mesh around the cushion ensuring a good definition of the boundary layer. The resulting mesh size consists of 60,000 cells. Adequacy of the mesh has been checked by performing a grid convergence study.

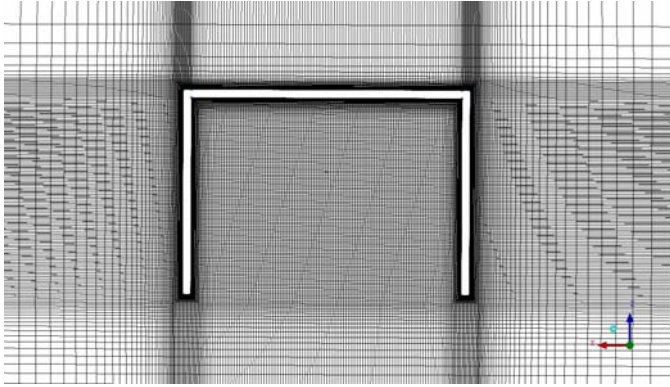


Figure 2 Detail of CFD mesh around the cushion

The total domain width is 30 times the width of the cushion. The sideways external boundaries of the domain are modeled with a Neuman condition for the velocity, a fixed average value of 1 atm for the pressure and a fixed free surface profile corresponding to the mean water elevation. In order to minimize the wave reflection phenomenon, a progressive coarsening of the grid cells in the spanwise direction away from the cushion is performed. The ambient air is modeled as an opening with constant pressure and the bottom of the basin as a non resisting wall.

The advection terms are discretized with the High Resolution Scheme which is a local blending between a first order upwind scheme and a second order central differencing. The time discretization is second order accurate and the time step is chosen to be 1/100 of the oscillation period. In order to ensure a significant reduction of the equation residuals and a good resolution of the strong non-linearities, at least 10 outer-loop iterations are performed per time step.

The results obtained with CFD are analogous to model tests and consist of time dependent physical data. Therefore, the extraction of derived quantities such as added mass and damping requires the same type of treatment. In this paper, they are computed using a least square fit of the filtered force and pressure time traces.

Effect of air compressibility

The compressibility of the aircushion (α) is related to the height of the cushion and may be computed by the following expression [21]:

$$\alpha = \frac{\rho g h_c}{\kappa P + \rho g h_c} \quad (1)$$

Where h_c is the height of the aircushion, κ is the gas law index (1.4 for air), and P is the air pressure inside the cushion.

According to this formulation the compressibility is 2% and may be neglected in the computations. In order to quantify more clearly the effect of compressibility on the simulations, a numerical check is required. The following matrix of

computations is performed at an oscillation frequency of 5.86 rad/s:

Table 2: Computation matrix for air compressibility study

Case	Standard case	Compressible air	Refined mesh	Compressible air + Refined mesh
Mesh size	60K	60K	110K	110K
Compressible air	NO	YES	NO	Yes

Since the mesh convergence study has only been done using incompressible air, there could be an effect of the mesh size on the results. This is why a finer mesh was tested in combination with compressible air.

Figure 3 shows the filtered time traces of the pressure for the considered cases. The added mass and damping coefficients calculated for each configuration are reported in Table 3.

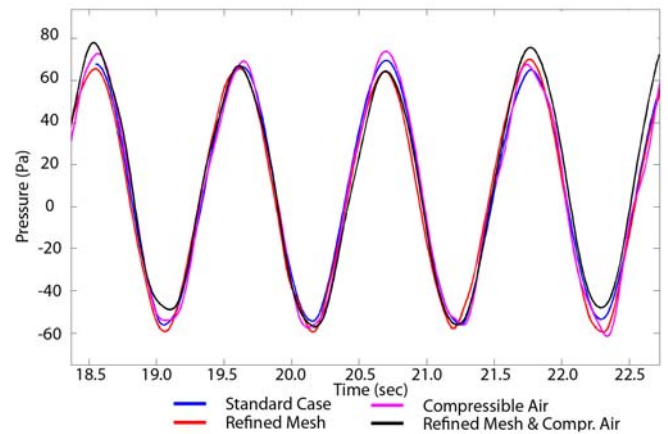


Figure 3 Filtered Force time traces

Table 3: Pressure and phase differences for different cases of the air compressibility study

	Standard case	Compressible air	Refined mesh	Compressible air + Refined mesh
P_0 (Pa)	59.442	61.230	60.094	61.328
ε (rad)	-15.711	-16.531	-15.326	-14.925

The time traces and derived coefficients show that the combined effects of air compressibility and mesh refinement account for less than 2% difference in the pressure amplitude and less than 1% for the phase angle. This is well within the precision of the filtering and least square methods used to determine the coefficients.

The main difference when using compressible air modeling lies in the computational time. It takes significantly more time for the pressure to converge toward an established regime when compressible air is used. This is due to high frequency oscillations appearing at the beginning of the simulation as can be seen in Figure 4. It takes a relatively long time before these

peaks are damped. Since the accuracy gain is negligible and the computational time increased, the conclusion of this preliminary check is to keep a fully incompressible model for both fluids for all the simulations.

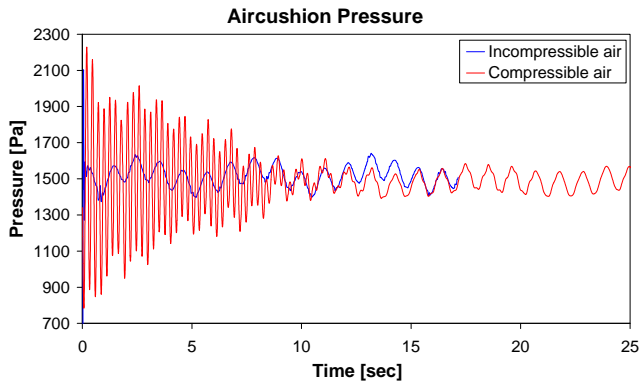


Figure 4: Time trace of the internal pressure inside the aircushion computed by CFD for heave oscillations of 1 cm at a frequency of 5.8 rad/s

3D POTENTIAL METHOD

Both the structure and the free surface inside each aircushion are modelled by panels. Two different panel models are constructed to show the influence of the panel size on the results. In both cases the structure is modelled by 364 panels, while the number of panels on the free surface inside the cushion is either equal to 120 or 480 panels. Figure 5 shows the model with 120 cushion panels.

A third potential computation was performed in which 3% of the critical damping was added to the cushion panels. In this case the structure and cushion were modeled by 364 and 120 panels respectively.

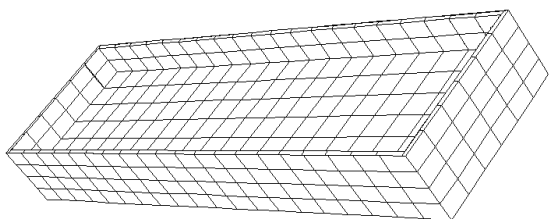


Figure 5: Panel model of the aircushion structure (upside down)

DISCUSSION OF RESULTS

Figure 6 to Figure 11 show the numerical and experimental results of the forced heave oscillations of the aircushion supported structure. Potential and CFD simulation were performed for a range of frequencies between 2.4 and 8.6 rad/s. It takes less than one second to compute one oscillating frequency with the present potential method. In general CFD computations are more time consuming. However the problem

was reduced to 2D. As a result the CFD simulations are relatively fast and the same computation with the CFD software takes on average 18 hours on a single 3 GHz processor.

The time trace of the aircushion pressure can be translated to a response amplitude operator (RAO) of the aircushion pressure variations as shown in Figure 6. Both Figure 6 and 7 indicate that numerical results are in good agreement with model tests. All data points are close together and the oscillation amplitude has no effect on the RAO of the pressure variations. In other words, there is a linear relation between air pressure variations and the oscillation amplitude.

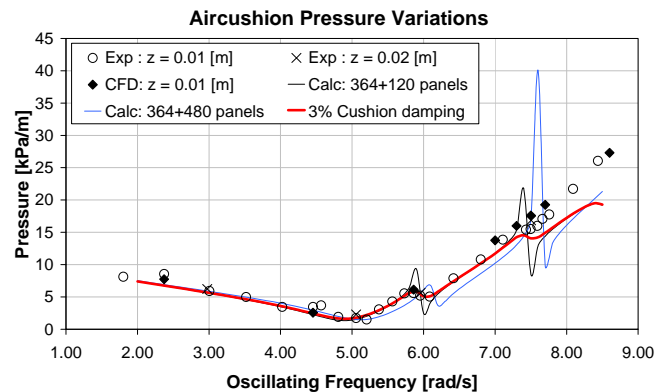


Figure 6: RAO of aircushion pressure variations

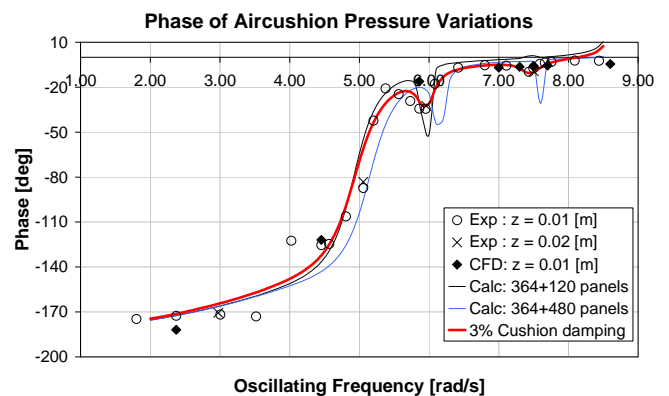


Figure 7: Phase of aircushion pressure variations

Contrary, the original potential formulation exhibits sharp variation peaks around 5.90 rad/s and 7.50 rad/s. These peaks are not present in the experimental results and encouraged a further investigation into numerical effects happening around these frequencies. For this reason CFD computations were performed and the potential method was modified to take into account additional damping of the cushion panels.

Results of the potential method show that the intensity and position of the peaks is affected by the mesh resolution which indicates that they are originated by cushion panel resonance. For high frequency oscillations larger than 7.40 rad/s, the potential calculations tend to underestimate the amplitude of the air pressure variations.

The introduction of additional damping to the cushion panels, being equal to 3% of the critical damping, does not affect the general trends while the peaks are filtered out. This leads to a better agreement with model tests. Although computed oscillation phase is in good agreement with model test data, the pressure amplitude is nevertheless still underestimated at high frequencies.

CFD results on the other hand are in good agreement with the experimental data over the total range of frequencies, both for phase and amplitudes of aircushion pressure variations. Remarkably, the reduction to a 2D model does not lead to major discrepancies with the experimental results.

Added mass and damping may be retrieved from the amplitudes and phase differences of the total pressure on the structure. The total pressure on the structure is almost equal to the pressure inside the cushion since the major part of the buoyancy is provided by the aircushion. Added mass and damping are presented in Figure 8 and Figure 9. It can be seen that these values are sensible to the differences in phase angles as was presented in Figure 7. During post-processing of the CFD results it was seen that a small difference in the raw data may lead to an important divergence in damping and added mass values. This explains why the agreement between experiments and computations is in some cases less good than the direct comparison of the amplitude and phase.

As a result, the general conclusions with respect to added mass and damping are the same as for the cushion pressure variations. Unphysical peaks predicted by the potential calculations are suppressed by additional damping but relatively larger discrepancies in the results still exist at high frequencies. CFD predictions are relatively accurate over the whole frequency range, but damping is under predicted at a frequency of 5.80 rad/s.

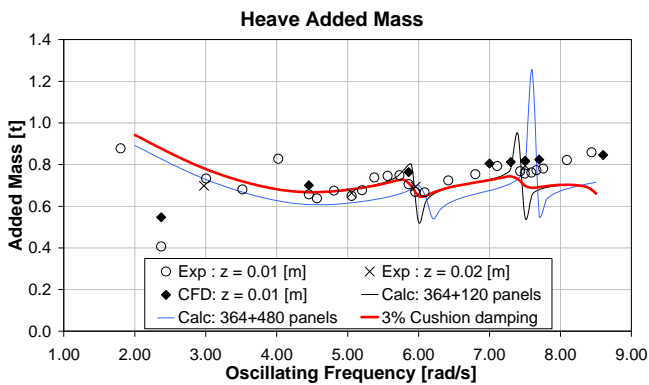


Figure 8: RAO of heave added mass

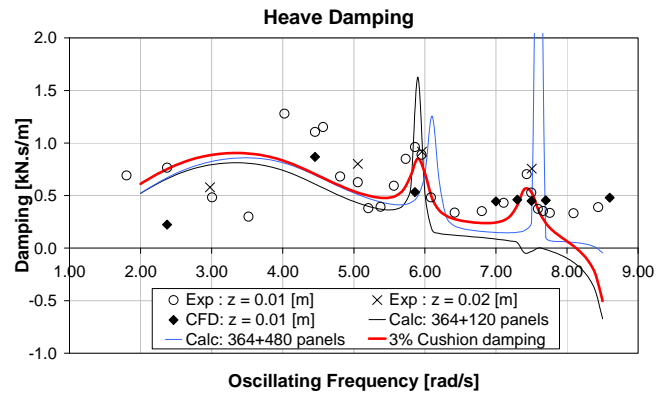


Figure 9: RAO of heave damping

It will be clear that air pressure variations inside the cushion are the result of the motion of the structure and water motions inside the aircushion. During model tests, wave elevations were also measured inside the aircushion near the centre of the structure. Figure 1 showed the location of these measurements. The RAOs of the wave elevations underneath the structure arising from the forced heave oscillations of the structure are presented in Figure 10. Figure 11 shows the corresponding phase differences. Experimental results show relatively high wave elevations around 6.00 and 7.50 rad/s, which are closely related to the increase of heave damping as indicated in Figure 9.

It can be seen in Figure 10 and 11 that there is a good agreement between both numerical methods and experimental results at low frequencies up to 5.00 rad/s. Although the potential method shows approximately the same trend as the measurements at higher frequencies, there is a significant difference in wave heights. CFD results on the other hand are fairly constant and in phase with the motion of the structure. The peaks in the amplitude of the wave elevations are not reproduced by CFD data.

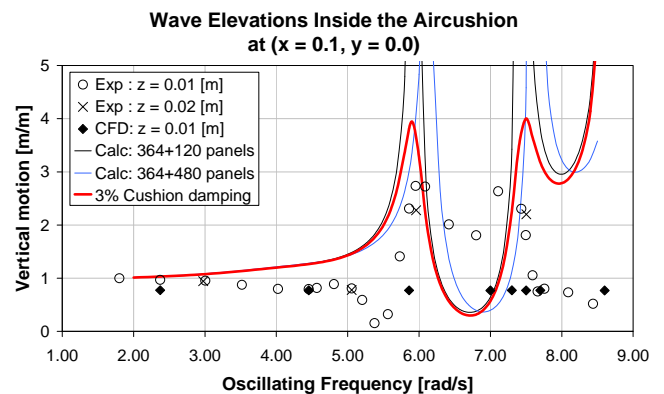


Figure 10: RAO of wave elevations inside the cushion at $(x = 0.1, y = 0.0)$

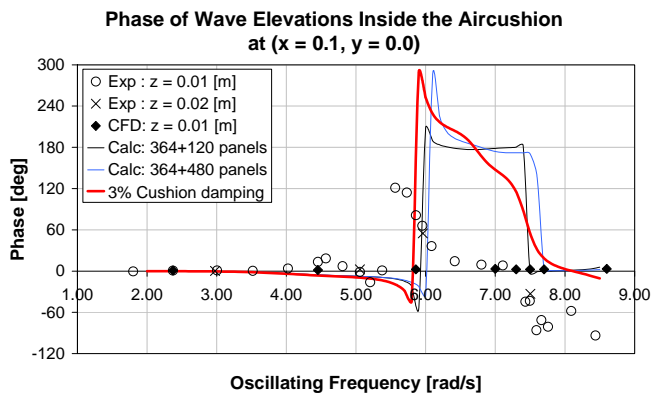


Figure 11: Phase of wave elevations inside the cushion at $(x = 0.1, y = 0.0)$

The wave height in the centre of the structure is dominated by the length of the cushion. Since only two dimensional transverse sections are taken into account in the CFD computations, it is impossible to accurately predict the wave height underneath the structure in case of relatively short waves. Figure 12 shows the vertical motions of the cushion panels which are the result of the potential calculations. This figure clearly illustrates that the wave heights underneath the structure are mainly influenced by the length of the cushion, rather than the width. Due to peaks in the wave elevation in the air chamber, the radiation damping is relatively high at 5.80 and 7.40 rad/s as was shown in Figure 9.

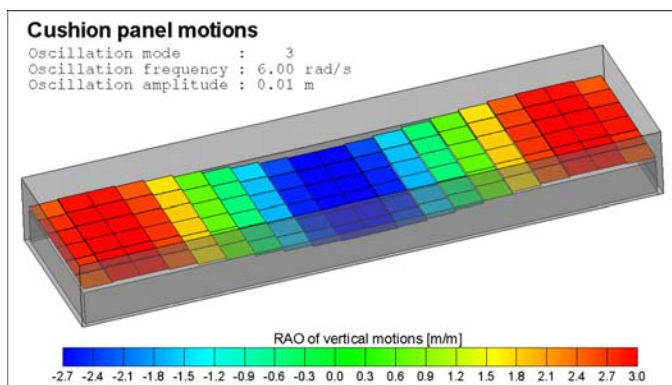


Figure 12: Vertical motions of cushion panels at 6.00 rad/s

CONCLUSION

The presented results show that the behaviour of an aircushion supported structure subjected to forced heave oscillations can be well predicted by both CFD and potential theory.

There is a good agreement between the numerical methods and experimental results for the aircushion pressure variation, added mass, damping and wave elevations inside the cushion. It was also shown that a linear relation between these quantities and the oscillation amplitude of the structure is justified.

In case of the potential method it was indicated that resonance effects of cushion panels may occur, which may efficiently be suppressed by additional damping. For aircushion supported

structures, improved potential calculations are an excellent tool to predict general trends and to obtain accurate results except at high oscillation frequencies.

In spite of strong modelling assumptions of a 2D incompressible problem, CFD results are in good agreement with model tests. It shows that CFD can be used confidently within the complete range of oscillation frequencies. The only discrepancies with model tests occur in the wave elevations underneath the structure. Potential calculations show that these are dominated by the cushion length which is not modelled in the 2D calculations. Therefore CFD emerges as a robust method allowing accurate simulations of forced heave oscillation of an air cushion supported structure, especially for high frequencies.

The difference in computational time between CFD and the presented potential method is significant. It takes less than one second to compute one oscillating frequency with in case potential theory is used. Conversely an average of 18 hours of computation time is needed before a statistical significant number of periods are computed with CFD.

This shows that the choice between CFD and potential modeling is a trade-off between accuracy and computational requirements, especially at high frequencies. Both methods are complementary having their respective advantages and drawbacks and may be used at different stages of the design process.

REFERENCES

1. CFX-5 Documentation, *Ansys*, Canada Ltd., 2004
2. Ikoma T, Masuda K, Maeda H, Rheem C-K. Hydroelastic Behavior of Air-Supported Flexible Floating Structures. *Proceedings of OMAE'02, ASME*, 2002.
3. Ikoma T, Maeda H, Masuda K, Rheem C-K, Arita M. Effects of Submerged Vertical Plates and Air chamber Units in Hydroelastic Response Reductions. *The Proceedings of The Twelfth International Offshore and Polar Engineering Conference*, 2002, pg. 547-552.
4. Ikoma T, Maeda H, Masuda K, Rheem C-K. Effects of the Air-chambers on the Hydroelastic Response Reduction. *Proceedings of International Symposium on Ocean Space Utilization Technology*, 2003, pg. 180-188.
5. Ikoma T, Masuda K, Rheem C-K, Maeda H, Iwasa R. Hydroelastic Behavior of Air-Supported Flexible Floating Structures. *Proceedings of OMAE'04, ASME*, 2004
6. Ikoma T, Masuda K, Rheem C-K, Maeda H. Three-dimensional analysis of hydroelastic behaviours of an aircushion type large floating structure. *Proceedings of OMAE'05, ASME*, 2005.
7. Ikoma T, Masuda K, Rheem C-K, Maeda H. Response Reduction of Motion and Steady Wave Drifting Forces of Floating Bodies Supported by Aircushions in Regular Waves. *Proceedings of OMAE'06, ASME*, 2006.
8. Ikoma T, Masuda K, Rheem C-K, Maeda H. Response Reduction of Motion and Steady Wave Drifting Forces of Floating Bodies Supported by Aircushions in Regular Waves - The 2nd Report, response characteristics in oblique waves. *Proceedings of OMAE'07, ASME*, 2007.

9. Ikoma, T., Kobayashi M., Masuda K., Rheem C.-K., and Maeda H. A prediction method of hydroelastic motion of aircushion type floating structures considering with draft effect into hydrodynamic forces. *Proceedings of OMAE'08, ASME*, 2008.
10. Lee, C.-H. and Newman, J.N. (2000). Wave Effects on Large Floating Structures with Air Cushions. *Journal of Marine Structures*, No. 13, 315-330.
11. Menter, F. Two-equation Eddy Viscosity Turbulence Models for Engineering Applications. *AIAA Journal*, 32, pp. 1299–1310. , 1994.
12. Pinkster, J.A. The effect of Air Cushions under Floating Offshore Structures. *Behavior of Offshore Structures, BOSS'97*, 1997, Vol. 8, pg. 143-158.
13. Pinkster, J.A. and Fauzi A. Motions and Drift Forces of Air-supported Structures in Waves. Fifth WEGEMT Workshop: Non linear Wave Action on Structures and Ships, September 1998
14. Pinkster, J.A., Fauzi, A., Inoue, Y. and Tabeta, S. The behaviour of large air cushion supported structures in waves," *Hydroelasticity in Marine Technology*, 1998, pp 497-506.
15. Pinkster, J.A. and Meevers Scholte, E.J.A. The behaviour of a large air-supported MOB at Sea. *Journal of Marine Structures*, 2001, No. 14, 163-179.
16. Raw, M. Robustness of coupled algebraic multigrid for the Navier-Stokes equations, *AIAA Paper 96-0297*, 1996
17. Tabeta, S., Model experiments on barge type floating structures supported by air cushions. Report 1125, *Laboratory of Ship Hydromechanics*, Delft University of Technology, Delft, 1998.
18. Thiagarajan, K. P. and Morris-Thomas, M. T. (2006). Wave-induced motions of an air cushion structure in shallow water. *Ocean Engineering*. Vol. 33, 1143–1160.
19. Tsubogo, T. and Okada, H. Hydroelastic Behavior of an Aircushion-Type Floating Structure. *Proceedings of ISOPE'02*, 2002.
20. Meevers Scholte, E.J.A. Mobile Offshore Base: Preliminary investigation on an Air Cushion Supported Mobile Offshore Base. *Delft University of Technology*, MSc Thesis.
21. Van Kessel, J.L.F. and Pinkster, J.A. The effect of aircushion division on the motions of large floating structures. *Proceedings of OMAE'07, ASME*, 2007.
22. Van Kessel, J.L.F. and Pinkster, J.A. The effect of aircushion division on the structural loads of large floating offshore structures. *Proceedings of OMAE'07, ASME*, 2007.
23. Van Kessel, J.L.F. and Pinkster, J.A. Wave-induced structural loads on different types of aircushion supported structures. *Proceedings of ISOPE'07*, 2007.
24. Van Kessel, J.L.F. Tuning the Air Pressure of Aircushion Supported Structures at Model Scale. *Proceedings of ISOPE'08*, 2008.
25. Van Kessel, J.L.F. Numerical and experimental study on aircushion supported structures. *Proceedings of OMAE'08*, 2008.
26. Wilcox, D. C. , *Turbulence Modeling for CFD*, 2nd ed. DCW Industries, 1998.